Surface Nanostructuring of TiO$_2$ Thin Films by Ion Beam Irradiation

P. Romero-Gomez[a], A. Palmero[a,1], F. Yubero[a], M. Vinnichenko[b], A. Kolitsch[b], A.R. Gonzalez-Elipe[a]

a) *Instituto de Ciencia de Materiales de Sevilla (CSIC-Universidad de Sevilla). c/ Americo Vespucio 49, 41092 Sevilla (Spain)*

b) *Institute of Ion Beam Physics and Materials Research. Forschungszentrum Dresden-Rossendorf, POB 510119, 01314 Dresden (Germany).*

Abstract.

This work reports a procedure to modify the surface nanostructure of TiO$_2$ anatase thin films through ion beam irradiation with energies in the keV range. The irradiation with N$^+$ ions leads to the formation of a layer with voids at a depth similar to the ion projected range. By setting the ion projected range few tens of nanometres below the surface of the film, well ordered nanorods appear aligned with the angle of incidence of the ion beam. Slightly different results were obtained by using heavier (S$^+$) and lighter (B$^+$) ions under similar conditions.

[1]Email: alberto.palmero@icmse.csic.es

Titanium dioxide (TiO_2) thin films possess outstanding properties that make them suitable for many technological applications. Their excellent optical transmittance, high refractive index, photoactivity, chemical stability, etc. have motivated the study of this material as well as the optimization of its properties and functionalities [1-2]. Within this context, surface nanostructuring of TiO_2 thin films turns out to be of great importance as the morphology of this material determines in a great extent many of its properties.

There are many examples of ion-beam-induced modifications of thin films in the literature [3]. For instance, Si and Ge thin films under He ion irradiation in the keV range develop microcavities in the material [4]. On the other hand, Ge, GaSb or InSb thin films show a so-called anomalous behaviour, i.e., they experience a clear swelling during the ion beam irradiation due to the formation of voids in the bulk [5-7]. These voids are formed as a result of the long-range migration of interstitial atoms and the movement of ion-induced point defects in the film [5]. Another remarkable effect has been reported for GaN thin films under ion beam irradiation. Here, an important stoichiometric imbalance takes place in the material due to the mass difference between ^{70}Ga and ^{14}N, producing Ga-rich and N-rich regions. Since many of these N atoms can not be easily incorporated into the network of the material, N_2 molecules are generated leading to the formation of nanometre-size bubbles embedded in the film [8-10]. Furthermore, there is evidence of migrating Ga interstitial atoms during the ion irradiation [11], thus suggesting a possible relation between the bubble formation mechanism and the ion beam induced movement of point defects. The mechanism for the bubble formation is still under research as there are cases of thin films containing randomly scattered N_2 molecules that do not come together and form a bubble.

Formation of scattered N_2 molecules embedded in thin films subjected to low energy N^+ implantation has been reported for different materials, such as GaN [12], SiO_X [13] and Al_2O_3 [14-15].

The behaviour of crystalline TiO_2 thin films under several tens keV ion beam irradiation has been extensively studied in the literature. It is known, for instance, that the TiO_2 network experiences an important depletion of oxygen due to the preferential sputtering [16-18]. To our knowledge, no indication of microcavities, anomalous swelling or bubble formation has been reported in the literature for TiO_2. The main aim of this letter is to study the interaction of ions with energies in the order of several tens keV with a TiO_2 anatase thin film to develop a systematic method to modify its morphology and nanostructure. In the course of this investigation, it has been shown that this technique can be used as a novel approach for the surface nanostructuring of this material.

TiO_2 thin films with thicknesses between 300 and 500 nm were deposited at 523 K using the plasma enhanced chemical vapour deposition technique. The films, depicting the anatase structure, showed a high degree of crystallinity and a clear columnar microstructure perpendicular to the substrate. The details of the structure, microstructure and other characteristics of the material as well as the description of the deposition technique appear in ref. [19]. In figure 1a-b, the cross-sectional and normal-view images of an as-deposited TiO_2 thin film obtained by scanning electron microscopy (SEM) are depicted. It consists of an arrangement of disordered grains agglomerated in the form of columns that extend from the substrate up to the surface. This microstructure will serve as a reference to compare with the results of the subsequent experiments. The ion irradiations were carried out at the Institute of Ion

Beam Physics and Materials Research, Forschungszentrum Dresden-Rossendorf. The ion fluence was always set to $2.4 \times 10^{17}\ cm^{-2}$, whereas the ion penetration depth and the ion projected range (R_P) were calculated using the SRIM software [20]. In the cases where the irradiation was carried out at room temperature, the ion current was set low enough to keep the film temperature below 70º C (340 K).

The TiO$_2$ thin film was firstly irradiated using a 60 keV N$^+$ ion beam impinging the surface at 45° to the normal. These conditions imply an ion PD of around 200 nm and a R_p of around 100 nm. This means an average concentration of implanted nitrogen of ~10^{15} ions cm^{-2} nm^{-1} in the film and few tens of nanometres of material removed due to the sputtering. The normal and cross-sectional SEM image of the TiO$_2$ thin film after irradiation appears in figure 2a-b. In figure 2b we have also depicted the calculated distribution of implanted ions in the film.

Figures 2a-b evidence three important differences compared with figures 1a-b: i) the columnar microstructure disappears in the implantation region, ii) the surface shows a very flat morphology, and iii) an intermediate layer containing spherical voids, with a diameter up to 10 nm, appears in the bulk of the material. The first feature can be understood by taking into account the ion-induced disorder in the material along the ion tracks, which also causes an important decrease of the crystallinity. This was corroborated by the loss of the X-ray diffraction (XRD) peaks observed for the original films (not shown). It is worth mentioning that the original columnar microstructure survives beneath the implanted region. The second feature indicates that the original pattern on the surface has been flattened: this phenomenon is well documented in the literature [21-22], where it has been explained by taking into consideration the

competition among ballistic effects, surface diffusion and thermal spike-induced volume viscous flow. The third feature in figure 2a-b, the appearance of a layer with nanometre-sized voids, is a remarkable phenomenon that, to our knowledge, is reported for the first time in the literature on TiO_2 thin films. Figure 2a shows a clear relation between the appearance of voids and the ion projected range (R_P depth) in the material. Thus, it seems that the migration of ion-generated point defects (responsible for the mentioned anomalous swelling of Ge, GaSb or InSb thin films) and/or the formation of N_2 bubbles into the material might play an important role in the formation of these voids. This issue will be discussed later on.

Figures 2a-b indicate that the microstructure of TiO_2 anatase thin films can be heavily modified through ion beam irradiation. Regarding the three abovementioned modifications produced by the N^+ ions, we propose a method to modify the film surface morphology: if the ion irradiation energy is set in such a way that R_P is close to the surface, apart from the well known processes responsible for the flattening of the surface (ballistic effects, surface diffusion and thermal spike-induced volume viscous flow), we will introduce a new competing mechanism (void formation) within the same spatial region. Thus, it is expected that this additional nanostructuring factor located in the top-most surface layers can affect the morphology of the film surface. This hypothesis is tested in the following experiments.

In figure 2c we depict the top-view and cross-sectional SEM images of a film irradiated with N^+ ions with an energy of 15 keV and an angle of incidence of 45 degrees, keeping the film temperature below 340 K during the irradiation. These conditions imply an ion penetration depth of 100 nm, and a R_P of about 50 nm. Figure 2c depicts a very different

morphology to that in figure 2a. In this case, a typical sponge-like disordered microstructure formed by nanometric elements that partially follow the direction of the ion beam is found. The cross-sectional SEM image (figure 2d) shows that the typical columnar structure of the original film remains in the non-implanted part, whereas tilted and disordered nanorods are formed in the surface region. The Raman spectrum of this film is shown in figure 3 along with the spectrum of a non-irradiated anatase TiO_2 material for the frequency range where the most intense TiO_2 anatase peak appears (i.e., 143 cm^{-1} corresponding to the E_g vibrational mode) [23]. This region is of particular interest because it provides important information about the structural changes of the material. The remaining part of the spectra is not shown as it provides redundant information about the anatase structure and has no relevance in this study. Comparing the two spectra in figure 3, we find two important differences: i) the peak corresponding to the irradiated film is broader than that of the non-irradiated one, and ii) the peak associated to the irradiated film shows a small shift towards higher wavenumber. In general, the variations of Raman peak shape are usually caused by surface tension of grains, nonstoichiometry, disorder induced by minor phases, or phonon confinement effects with the grain size variation. However, for TiO_2 it was demonstrated that the changes observed in the Raman spectra were not related to any internal stress or grain size effects [23]. Thus, the redshift of the spectrum can only be linked to the increase of lattice parameter (loss of crystalinity), and the subsequent decrease of the phonon frequency, as well as to the presence of dangling bonds associated to the oxygen depletion [23]. This latter effect is expected due to the aforementioned preferential sputtering of oxygen atoms during irradiation, and agrees with the fact that the film becomes dark coloured and shows a high electrical conductivity, both features typical of partially reduced titanium oxide materials.

In order to allow the film to recrystallize during the ion bombardment, we performed an experiment similar to the previous one, i.e. we irradiated with N^+ ions with an energy of 15 keV and an angle of incidence of 45º, but this time we set the film temperature to 700 K during the ion irradiation. These conditions ensure the recrystallization of the film into the anatase phase. The normal and cross-sectional SEM images depicted in figures 4a-b correspond to this experiment. As in the previous case, the cross-section view depicts a typical columnar microstructure in the bottom part of the film. However, now the film termination consists of well ordered nanorods formed in the ion penetration depth region. Thus, in figure 4a, presenting the normal-view in two scales, a regular pattern of nanorods with similar width ranging between 20 and 30 nm can be observed on the surface. The cross-sectional view (figure 4b) shows that the nanorods have a length of approximately 100 nm and that they are quite well aligned along the ion beam direction. In figure 3, the Raman spectrum of this film shows a sharper peak than that of the equivalent sample irradiated at room temperature, indicating a better crystallinity of the film [23], which is expected due to the higher film temperature during irradiation. This agrees with XRD measurements where the peaks of the anatase structure of titanium oxide could be detected (not shown).

To know more about the proposed method for the modification of the surface topography, we performed another experiment using an ion with a similar atomic mass as nitrogen but that in no way can produce gas bubbles into the layer. Thus, we irradiated the TiO_2 thin film with a B^+ ion beam with an energy of 30 keV and an angle of incidence of 45º. The film temperature was kept equal to 700 K during the irradiation to allow recrystallization. Under these conditions, the ion penetration depth was 120 nm

and R_P 60 nm, quite similar to the previous experiments with nitrogen. The normal-view SEM image of the irradiated film is depicted in figure 4c, showing different features than in the previous cases. This time small cavities are formed on the surface of the film, and no hint of nanorod formation is found. This becomes more evident in figure 4d, where we depict the cross-sectional SEM image. Thus, this situation seems to represent an intermediate state where voids are formed on the surface of the material while other mechanisms are responsible for the flattening of the remaining surface regions. The Raman spectrum of this film also appears in figure 3, and is characterized by a larger shift of the peak towards the right when compared with the non-irradiated spectrum. This points out that the reduction of the material due to the preferential sputtering of oxygen is much larger than that during nitrogen irradiation. The distinct chemical character of nitrogen and boron in the implanted state may also contribute to this difference: nitrogen is a very electronegative atom that tends to form nitride species when it is combined with metals, whereas boron may act as a cation when it is bonded to oxygen. Hence, different chemical structures are expected when they are implanted in TiO_2.

In a last experiment we employed a heavier ion, S^+, performing the irradiation with an angle of incidence of 45° and an energy of 45 keV, keeping the film temperature equal to 700 K. Thus, the ion penetration depth was about 50 nm, and R_P 30 nm. The normal-view SEM image of the film after irradiation with the S^+ ion is shown in figure 4e, where we can find spaced structures similar to those in figure 4a. The cross-sectional SEM view of the film (figure 4f) shows that the surface is completely covered with nanorods aligned with the ion beam, although this time they are sharper and slightly less ordered than those formed by the nitrogen irradiation. Regarding the Raman spectrum

(figure 3), we find a clear shift of the peak towards the right as compared with the non-irradiated case. As we noted previously, this shift reveals a significant reduction of the oxide thin film [23].

This experiment with S^+ ions suggests that the formation of nanorods on the surface of the film, and thus the formation of voids during ion irradiation, is mainly associated to the migration of point defects during the irradiation and not to the formation of bubbles. This is supported by the fact that implanted S^+ cannot be released as a gas and must remain as defect ions within the TiO_2 structure. The different behaviour found with B^+ suggests that a certain threshold for the momentum and energy deposited on the TiO_2 and the different chemical character of the species are also important factors controlling the formation of nanorods. Our previous results, showing that ordered nanorods are only formed at 700 K also suggest that thermally activated diffusion is also important for these processes. Although this temperature is not very high for the mobilisation of stoichiometric TiO_2, it can be sufficient for the mobilisation of an oxygen depleted titanium oxide: the so called Magnelli phases (i.e., Titanium Oxides with a variable stoichiometry of the type TiO_x, x<2) are well known for their high mobility at not very high temperatures [24]. Similarly, for anatase films, a high mobility of Ti^{3+} species from the bulk to the surface has been directly observed using the scanning tunneling microscopy technique on partially reduced single crystals of this material heated in vacuum [25]. No further conclusion on the fundamental mechanisms responsible for the surface nanostructuring under ion irradiation can be achieved regarding our experiments, and more research, out of the scope of this letter, is required. However, from a phenomenological point of view, it seems that the parameters that determine the appearance of nanorods on the surface of the film are the ion penetration depth, the

deposited amount of momentum and energy, the reduction of the network, and the thin film temperature during irradiation. Moreover, in the case of N^+ ion implantation we can not rule out the presence of N_2 bubbles in the material.

Summarizing, the previous results indicate that ion beam irradiation in the keV range can be employed to change the surface morphology of a TiO_2 thin film in a similar way as for the cellular structures reported for Ge, GaSb or InSb thin films [5] or other materials [26]. For TiO_2, the formation of well ordered nanorods as those shown in figures 4a-b and 4e-f can be of the outmost importance for the improvement of the photocatalytic, photovoltaic or sensor [27] properties aimed for nanostructured TiO_2 thin films. Furthermore, the controlled formation of surface nanorods could be important for the improvement of the TiO_2 capabilities as electron collector or to enhance its sensitivity to gases.

References

[1]   O. Carp, C.L. Huisman, A. Reller, Prog. Sol. Stat. Chem. **32** (2004) 33

[2] A. Fujishima, T.N. Rao, D.A. Tryk, J. Photochem. Photobiol. C: Photochem Rev. **1** (2000) 1.

[3] A.R. Gonzalez-Elipe, F. Yubero and J.M. Sanz, Low Energy Ion Assisted Film Growth, Imperial College Press 2003.

[4] S.M. Myers, D.M: Follstaedt, G.A. Petersen, C.H. Seager, H.J. Stein, W.R. Wampler, Nucl. Inst. Meth. Phys. Res. B **106** (1995) 379

[5] N. Nitta, M. Taniwaki, Y. Hayashi, T. Yoshiiem J. Appl. Phys, **92(4)** (2002) 1799

[6] R. Callec, P.N. Favennec, M. Salvi, H.L'Haridon, M. Gauneau, Appl. Phys, Lett. **59(15)** 1991 1872.

[7] D. Kleitman and H.J. Yearian, Phys. Rev. **108** (1957) 901

[8] S.O. Kucheyev, J.S. Williams, C. Jagadish, J. Zhou, V.S. J. Craig, G. Li, Appl. Phys. Lett. **77(10)** (2000) 1455

[9] S.O. Kucheyev, J.S. Williams, J. Zhou, C. Jagadish, G. Li, Appl. Phys. Lett. **77(22)** (2000) 3577

[10] S.O, Kucheyev, J. E. Bradby, C.P. Li, S. Ruffell, T. van Buuren, T.E. Felter, Appl. Phys. Lett. **91** (2007) 261905

[11] W. Jiang, Y. Zhang, W.J. Weber, J. Lian, R.C. Ewing, Appl. Phys. Lett. **89** (2006) 021903

[12] B.J. Ruck, A. Koo, U.D. Lanke, F. Budde, S. Granville, H.J. Trodahl, A. Bittar, J.B. Metson, V.J. Kennedy, A. Markwitz, Phys. Rev. B **70** (2004) 235202

[13] J.P. Holgado, A. Barranco, F. Yubero, J.P. Espinós, A.R. Gonzalez-Elipe, Nucl. Instr. and Meth. in Phys. Res. B **187** (2002) 465

[14] J.P. Holgado, F. Yubero, A. Cordon, F. Gracia, A.R. Gonzalez-Elipe, J. Avila, Solid State Comm. **128** (2003) 235

[15] J.P. Espinos, A.R. Gonzalez-Elipe, M. Mohai, I. Bertoti, Surf. Interf. Anal. **30** (2004) 90

[16] R. Asahi, T. Morikawa, T. Ohwaki, K. Aoki, Y. Taga, Science **293** (2001) 269

[17] M. Takeuchi, Y. Onozaki, Y. Matsumura, H. Uchida, T. Kuji, x Nucl. Instr. And Meth. in Phys. Res. B **206** (2003) 259 .

[18] N. Ishikawa, S. Yamamoto, Y. Chimi, Nucl. Instr. and Meth. in Phys. Res. B **250** (2006) 250

[19] A. Borras, C. Lopez, V. Rico, F. Gracia, A.R. Gonzalez-Elipe et al, J. Phys.

Chem. C **111** (2007) 1801

[20]   http://www.srim.org/

[21]   S. Vauth, S.G. Mayr, Phys. Rev. B **77** (2008) 155406

[22]   P. Mishra and D. Ghose, Nucl. Inst. Meth. Phys. Res. B 266 (2008) 1635

[23]   J.C. Parker and R.W. Siegel, Appl. Phys. Lett. **57(9)** (1990) 943

[24]   L. Liborio and N. Harrison, Phys. Rev. B 77(10) (2008) 104104

[25]   M. Bowker, Phys. Chem. Chem. Phys. 9 (2007) 3514

[26]   S.M. Allameh, N. Yao, W.O. Soboyejo, Scripta Mater. **50** (2004) 915

[27] S.E. Gledhill, B. Scott, B.A. Gregg, J. Mater. Res. **20** (2005) 3167.

Figure Caption

Figure 1. Images of non-irradiated TiO_2 thin films obtained using SEM: a) non-irradiated sample, cross-sectional view, b) non-irradiated sample, normal view.

Figure 2.- Images of irradiated TiO_2 thin films with an angle of incidence of 45º and at room temperature obtained using SEM: a) N^+ ions with an energy of 60 keV, top-view, b) N^+ ions with an energy of 60 keV, cross-sectional view along with the calculated implantation profile, c) N^+ ions with an energy of 15 keV, normal view, and d) N^+ ions with an energy of 15 keV, cross-sectional view (the region of interest is framed). The substrate position is at the bottom of the cross-sectional images.
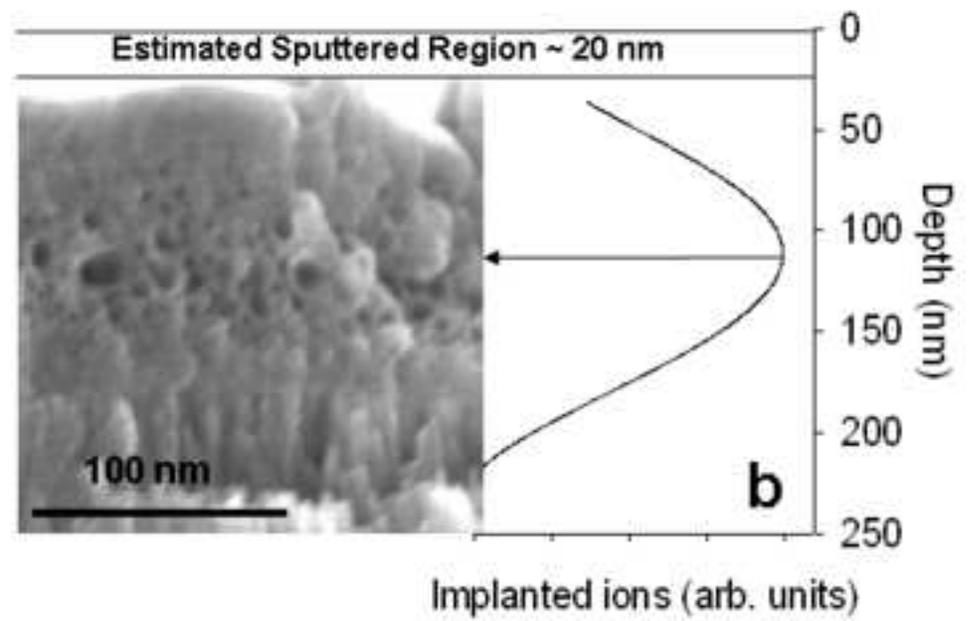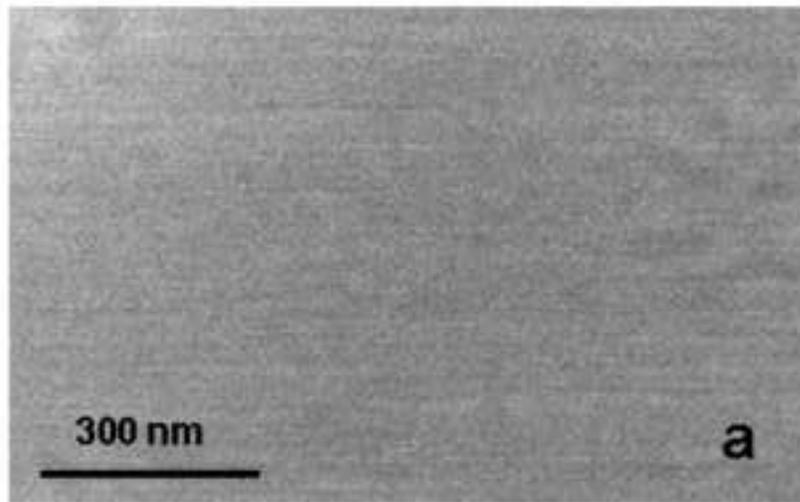
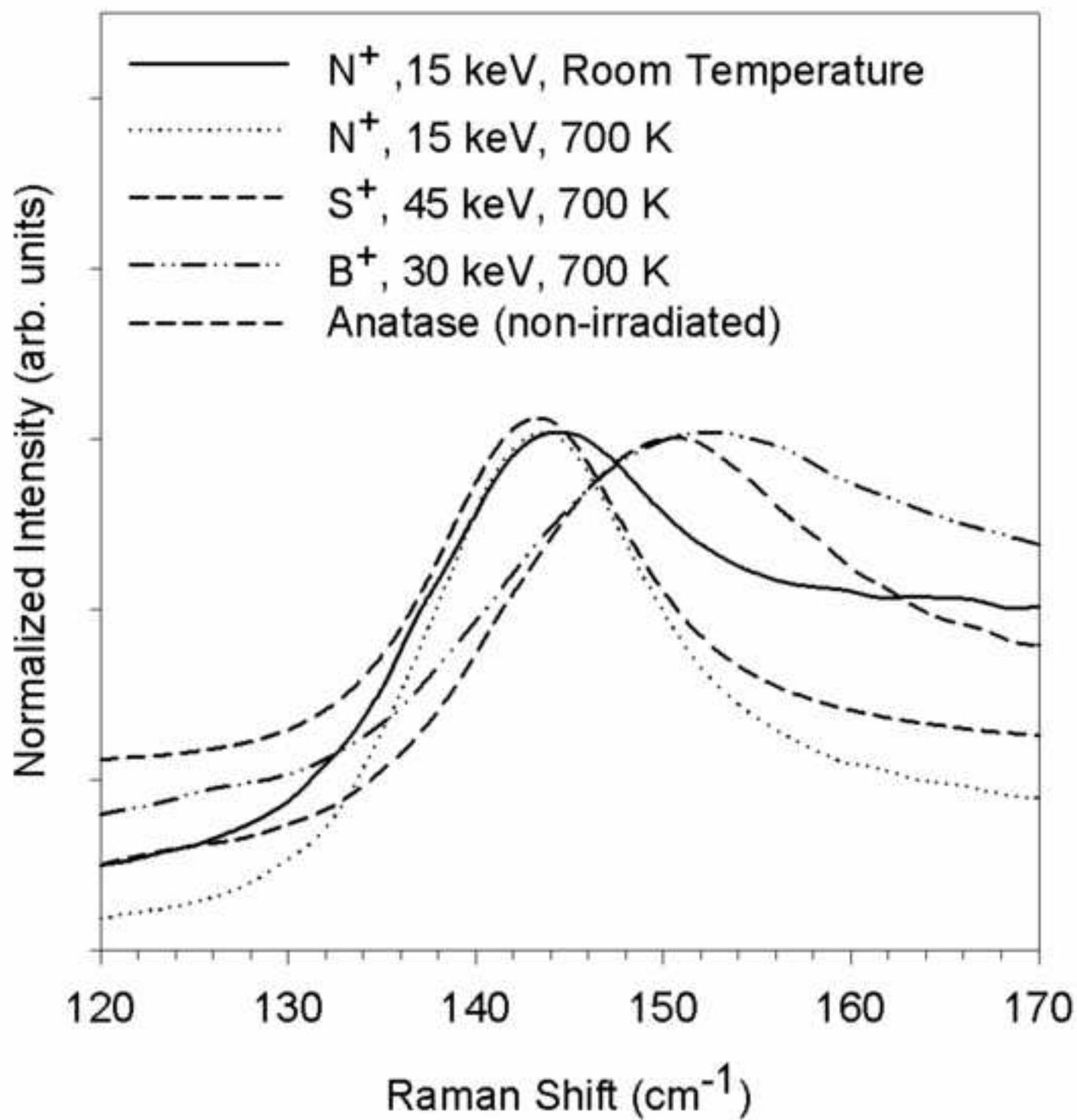Figure 3.- Raman spectra of TiO_2 thin films under different irradiations.

Figure 4.- Images of irradiated TiO_2 thin films with an angle of incidence of 45º and at 700 K obtained using SEM: a) N^+ ions with an energy of 15 keV, normal view, b) N^+ ions with an energy of 15 keV, cross-sectional view, c) B^+ ions with an energy of 30 keV, normal view, d) B^+ ions with an energy of 30 keV, cross-sectional view, e) S^+ ions with an energy of 45 keV, normal view, f) S^+ ions with an energy of 45 keV, cross-sectional view. The black arrow indicates the angle of incidence of the ions. The substrate position is at the bottom of the cross-sectional images.

Estimated Sputtered Region ~ 20 nm

Depth (nm)

Implanted ions (arb. units)

300 nm

a

100 nm

b

300 nm

c

100 nm

d